Stereoselectivity Behavior of the AZ28 Antibody Catalyzed Oxy-Cope Rearrangement†

Sergio Martí,‡ Juan Andrés,‡ Vicent Moliner,*,‡ Estanislao Silla,‡,§ Iñaki Tuñón,*,§ and Juan Bertrán#

Departament de Ciències Experimentals, Universitat Jaume I, Box 224, Castellón Spain, Departament de Química Física/ IcMol, Universidad de Valencia, 46100 Burjasot, Spain, and Departament de Química, Universitat Autònoma de Barcelona, 08193 Bellaterra, Spain

Received: August 19, 2005; In Final Form: November 2, 2005

Catalytic antibodies are very interesting not only because of the rate enhancement of the reactions that they catalyze but also because of the selectivities they can achieve that are sometimes not present in natural enzyme processes. We have selected the study of the stereoselectivity of the matured AZ28 that catalyzes an oxy-Cope rearrangement. For this particular case, the presence of a chiral center in the substrate provokes the existence of two different enantiomers, *R* and *S*. Furthermore, it is also possible to locate two different orientations for the hydroxyl group in the central ring of the substrate in the transition state, equatorial and axial, rendering two different conformers. In this paper we present the free energy profiles obtained for different substrate isomers in the cavity created by the matured catalytic antibody. Our simulations have reproduced the stereoselectivity of the matured AZ28, differentiating between the axial or equatorial orientations and preferentially stabilizing the S forms, at a qualitative level. Finally, the inclusion of the substrate−CA interactions in a flexible molecular model has allowed us to observe the different pattern of interactions that are related to different interaction energies, which seem to be crucial in the stereoselectivity behavior of the catalytic antibody.

1. Introduction

Catalytic antibody (CA) design is a highly fashionable topic since the first one was elicited against a transition state analogue (TSA) three decades ago.[1] The immune system can recognize and produce antibodies for any molecule. The most abundant monoclonal antibodies, the immunoglobulin proteins, consist of two identical light chains and two identical heavy chains connected by disulfide bridges. Both chains have a constant domain and a variable one, which is the antigen-recognizing site composed of the variable region of both chains.[2,3]

The decrease of the activation barrier in an enzymatic process arises from the larger binding energy of the transition state (TS) with respect to the reactants (Michaelis complex, MC).[4] These ideas can be translated to antibodies programming the immune response to a stable molecule that mimics the presumed structural and electronic features of the TS of a particular reaction; the TSA. Thus the hapten to be used will be this particular stable molecule. Due to its flexibility a significant reorganization of the germline CA active site occurs upon ligand binding.[5] In the maturation process, the optimal active site conformation is fixed, increasing the affinity for a particular antigen. The result should be the evolution of the antibody binding site with maximum complementarity to the TSA and, hopefully, to the TS.

Although CAs have been produced for a plethora of chemical reactions, as a general feature, the catalytic power of CA is never as high as the one obtained in enzymes (k_{cat}/k_{uncat} being 10^6 in CA and up to 10^{17} in enzymes).[6] Furthermore, not all antibodies that stabilize TSAs are catalysts of the reaction and, what is more intriguing, there are cases where after a process of maturation (that yields an increased affinity of the CA for the TSA) a paradoxical decrease in the catalytic power is observed, with respect to the initial or germline CA.[7] Considering that the maturation processes always increase the affinity of the CA by the TSA, and assuming that this structure is close to the TS, an increase in the rate catalytic power of the CA should be expected in the mature form, as normally observed.

The oxy-Cope rearrangement catalyzed by AZ28[7] is an extremely interesting system because no enzyme is known for this reaction. The monoclonal AZ28 catalyzes the unimolecular rearrangement of a substituted hexadiene to an enol that spontaneously proceeds to the corresponding aldehyde (see Scheme 1). As can be observed in the scheme, the TSA presents a chairlike structure in the substituted cyclohexanol, similar to the structure of the TS. Nevertheless, there is also a difference that is the hybridization of the C2 and C5 atoms of the central ring; although these two carbon atoms in TSA are sp^3, the hibridization of the equivalent atoms in the TS of the reaction is sp^2.

From the germline antibody, generated against this TSA, a matured AZ28 form was obtained after six different mutations; four of them in the heavy chain and two in the light one. Only one of these mutations, SerL34Asn, is located in the active site. The result of these mutations is that in the case of the AZ28, it was found that the matured AZ28 presents a 40-fold higher affinity for the TSA but affords a 30-fold lower rate enhancement than its germline precursor.[7] The aforementioned mutation on the active site seems to be largely responsible of the decrease of the catalytic efficiency of the antibody. This paradoxical

† Part of the special issue "Donald G. Truhlar Festschrift".

* Corresponding authors. V.M.: tel, +34964728084; fax, +34964728066; e-mail, moliner@exp.uji.es. I.T.: tel, +34963544880; fax, +34963544564; e-mail, Ignacio.Tunon@UV.es.

‡ Universitat Jaume I.

§ Universidad de Valencia.

Universitat Autònoma de Barcelona.

10.1021/jp054679a CCC: $33.50
Published on Web 12/22/2005

SCHEME 1: Schematic Diagram of the Molecular Mechanism of the Oxy-Cope Reaction from the Substituted Hexadiene, MC, to the Enol, P, through a Transition State, TS[a]

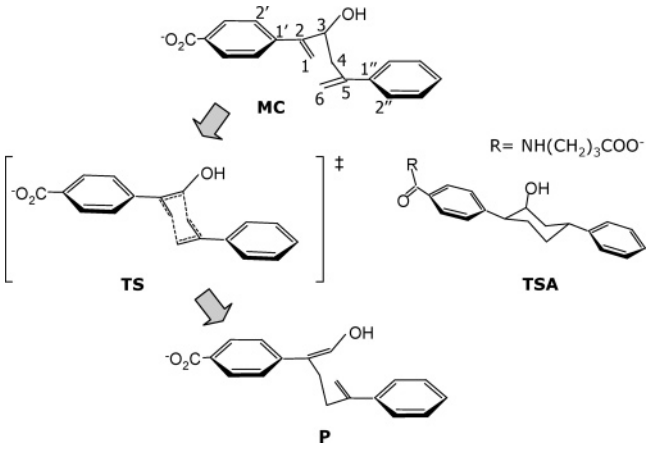

[a] A detail of the **TSA** is also depicted for comparison.

behavior of the AZ28 has been previously addressed in three theoretical papers.[8−10] In the paper of Kollman and co-workers,[8] binding free energies between AZ28 and the hapten were calculated using the molecular-mechanics-Poisson−Boltzmann/surface area (MM-PB/SA) method developed by Srinivasan et al.[11] to demonstrate the negative correlation between TSA binding affinity and the catalytic rate of the CA. The binding free energies were calculated from snapshots taken at intervals from trajectories of each AZ28−hapten complex, for both the germline and the matured CA forms. The energetic analysis was done for only a single molecular dynamics (MD) trajectory of the desired antibody−hapten complex with unbond antibody and hapten structures taken from snapshots of that trajectory. Due to the fact that classical MD calculations are run for TS complexes, reactants and TS structures optimized in the gas phase were used to make additional force field parameters for the MM-MD simulations. In the work of Houk and co-workers,[9] a more complete study of the reaction in the gas phase at the B3LYP level is carried out. Flexible ligand docking in rigid germline and matured antibodies allows discussion of the stereoselectivity of the reaction. Finally, in our previous paper,[10] a quite different strategy through free energy profiles using an appropriate distinguished reaction coordinate is employed. This procedure leads to a more accurate estimation of the free energy variation along the reaction coordinate taking also into account the flexibility of the CA. The free energy profiles obtained in the germline and the matured CA, as well as in solution, were in very good agreement with experiments. An analysis of the difference between the germline and the matured suggested that the change in the pattern of interactions between the TS and the reactants in the matured form was responsible for the difference in the activation free energies.

The applicability of CA in organic synthesis relies on the fact that they are both efficient and very selective.[12,13] CA can be very interesting because they can achieve selectivities that are sometimes not present in natural enzymes.[13] In the case of AZ28, the presence of a chiral center in the substituted hexadiene molecule (the C3 atom in Scheme 1), which is the substrate of the oxy-Cope rearrangement catalyzed by this CA, provokes the existence of two different enantiomers, R and S. These two enantiomers were separated by reversed phase chiral HPLC and then assayed individually for catalysis by the CA. The stereochemical kinetic preference of the matured AZ28 for the S enantiomer of the substrate was observed,[14,15] the ratio between the rate constant of the *S* and *R* enantiomers (k_{cat}^{S}/k_{cat}^{R}) being 15.1.[16] Furthermore, it is also possible to locate two different orientations for the hydroxyl group in the central ring in the TS: equatorial and axial. Previous gas-phase calculations have revealed that the preference for this reaction through a transition state with an axial or equatorial hydroxyl group depends on the electronic character of the substrate; the axial conformation is preferred for the protonated substrate whereas the equatorial structure is the most stable one for anionic substrate.[9] The prediction carried out by Houk et al.[9] in this sense was that the nonpolar environment created by the CA closely resembles the gas-phase calculations and, consequently, the reaction should proceed through an equatorial TS enantiomer.

In this paper we will present the free energy profiles, in terms of potential of mean force (PMF), obtained for different substrate conformers in the cavity created by the matured CA applying the same strategy carried out in our previous paper.[10] The stereoselectivity of the matured AZ28 CA, differentiating between the axial or equatorial orientations and preferentially stabilizing the *R* or *S* forms, will be discussed and analyzed in this paper.

2. Computing Methods

The starting point for the PMF calculations was obtained from the TSA−CA X-ray coordinates.[17] The structure of the hapten was slightly modified to obtain a TS-like structure, keeping fixed the positions of the C2 and C5 atoms, to avoid large variations in the position of the phenyl rings due to the change of the hybridization of these atoms. The resulting structure was then relaxed by means of 500 ps of MD simulations, applying a harmonic constraint on the distances of the breaking and forming bonds. The simulated system consisted of a cubic box of 79.5 Å per side with the CA and 15 492 water molecules (50 167 atoms in total) all treated using the OPLS-AA force field,[18] plus the substrate (39 atoms) that was treated by AM1 semiempirical Hamiltonian. Because of its size, those CA residues lying outside a sphere of 32 Å of radius centered in the substrate center of mass were removed and the atoms lying inside a sphere of 30 Å of radius were allowed to move (∼11 500 atoms), keeping frozen the position of the rest. The final structure was refined by means of a TS search, confirming the presence of only one negative eigenvalue in a reduced Hessian matrix that contains the coordinates of the substrate. The resulting structure was the *R*-equatorial TS enantiomer. Using this structure, an initial guess for the *S*-axial TS simulations was obtained interchanging the position of the −OH and −H substituents of the C3 atom. To obtain an initial configuration of the *S*-equatorial TS, the intermediate ring was rotated around the axis containing the C2 and C5 atoms. The same operation was carried out from the *R*-equatorial conformer to obtain an initial structure of the *R*-axial TS. A total of 500 ps of NVT Langevin−Verlet dynamics calculations were run for the antibody−TS structures applying harmonic constraints on the distances of the breaking and forming bonds. The time step was 1 fs, the temperature was 300 K, and the switched cutoff radius applied to all the interactions was 12 Å. In this way, the TSs were fitted into the active site, allowing the relaxation of not only the chemical system but also the antibody.

Free energy profiles for the different isomers in the CA were obtained as a PMF appearing along a distinguished reaction coordinate, obtained as the antysimmetric combination of the C1−C6 and C3−C4 distances.[10] Selection of this reaction coordinate is based on the exploration of the potential energy

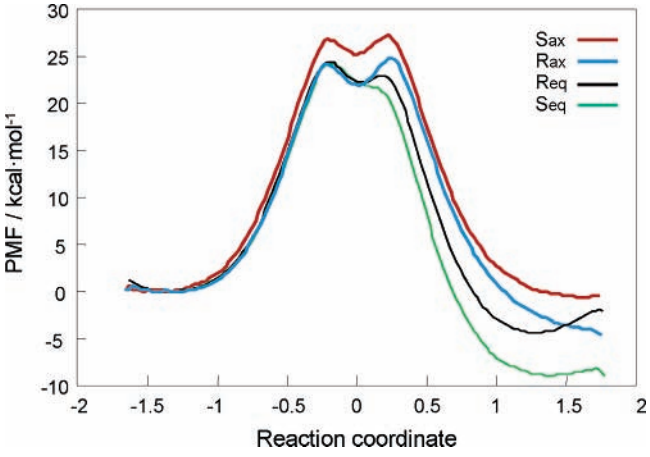

Figure 1. Free energy profiles (in terms of PMF) for the AZ28 catalytic antibody in its matured form for the *S*-axial (red line), *R*-axial (blue line), *R*-equatorial (black line), and *S*-equatorial (green line) conformations for the MC to P transformation (see Scheme 1). The reaction coordinate is the anti-symmetric combination of the interatomic distances of the forming and breaking bonds, C1···C6 and C3···C4, respectively.

surface (PES) including the environment by means of the reaction paths traced down to the corresponding reactants and products valleys from transition structures located and characterized in the CA active site. The axial and equatorial labels for the two reactant complexes that were obtained from their corresponding TSs will be maintained although, in a rigorous manner, they cannot be classified in these categories because there is no central ring in the reactants. Simulations were carried out with the DYNAMO program[19] based on the original idea of the hybrid quantum mechanical/molecular mechanical (QM/MM) methods.[20] All the degress of freedom were sampled by means of a series of molecular dynamic simulations. Umbrella sampling[21] was used to place the chemical system at different values of the reaction coordinate that cannot be enough frequently sampled by thermal fluctuations and then molecular dynamics simulations were run. This is done by adding an adequate parabolic energy function centered at the value of the reaction coordinate that is being explored. The fluctuations of the reaction coordinate are finally pieced together by means of the weighted histogram analysis method, WHAM,[22] obtaining the full distribution function and thus the PMF profile. A total of 72 simulation windows were needed to sample the whole range of the distinguished coordinate. At each window, 3 ps of equilibration were followed by 10 ps of production. As before, we used Langevin−Verlet dynamics with a time step of 1 fs and the temperature of the bath was 300 K. The umbrella force constant was of 2500 kJ·mol^{-1}·Å^{-2}.

Once the full PMFs were obtained, additional MD trajectories of 1 ns were carried out in the region of the TS (with harmonic constrains applied just in the reaction coordinate) and MC, using the same simulation protocol as described above. A decomposition of the averaged total potential energy as the sum of the QM energy, the QM/MM interaction energy and the MM energy ($E = E_{QM} + E_{QM/MM} + E_{MM}$) has been carried out as already done in previous studies for the [3,3] sigmatropic rearrangement catalyzed by chorismate mutase.[23,24]

3. Results

The resulting PMFs obtained for the *S* and *R* enantiomer substrate, for both the axial and equatorial orientations of the hydroxyl group of the substituted hexadiene intermediate ring, are presented in Figure 1. The free energy barriers for the *S*-axial and *S*-equatorial are 26.8 and 24.2 kcal·mol^{-1}, respectively. This difference of 2.6 kcal·mol^{-1}, that describes a more favorable reaction in the later, reveals a stereoselectivity in the AZ28. This behavior is also reflected in the free energy barriers corresponding to the R enantiomer, 24.4 kcal·mol^{-1} for the *R*-equatorial and 24.9 kcal·mol^{-1} for the *R*-axial. It can be observed that, although very slightly, the *S*-equatorial is the most favorable enantiomer, reproducing the experimental trend.

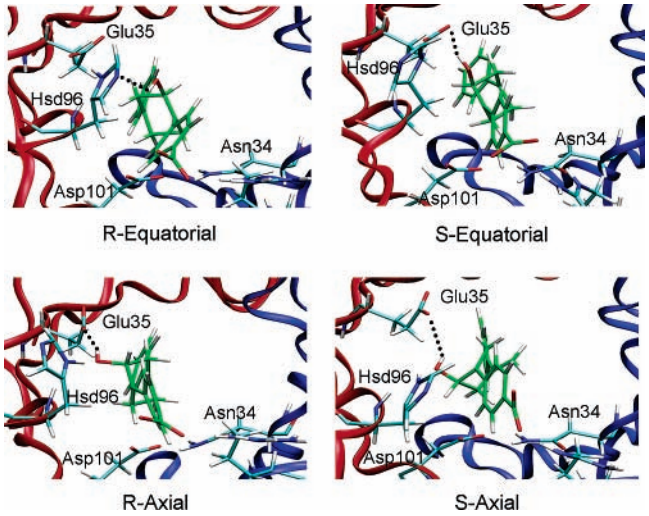

Figure 2. Detail of the averaged structures of the four different conformers of the TS oxy-Cope rearrangement in the active site of the matured AZ28 antibodies.

Averaged structures of the TSs obtained for the four different enantiomer are presented in Figure 2 and the most important geometrical internal coordinates, averaged over the last 500 ps of the dynamics listed in Table 1. First of all, it is important to mention that the interaction between the hydroxyl group and proton acceptor groups of the protein has been demonstrated to be determining in the catalytic power of the CA.[10] In this regard, the hydroxyl substituent in the *S*-equatorial and *R*-axial enantiomer TS structures is interacting with the Glu-H35 more strongly than in the *S*-axial and *R*-equatorial, thus presenting the same pattern of interactions than in the TSA,[10] although with larger intermolecular distances. The shorter OH···Glu-H35 distance present in the *S*-equatorial and *R*-axial is related to a larger distance between the same hydroxyl group and the Hsd-H96. A different interaction of the hydroxyl group with the Asp-H101 has been previously proposed by Houk et al.[9] Nevertheless, in our simulations this later residue is interacting in all cases with the Asn-L34, instead. There are experimental evidences that the germline has a larger cavity than the one observed in the matured form,[17] which can be monitored through the distance between these two residues that are located in the outer part of the catalytic cavity;[10] although the matured isomers presented in Table 1 are around 2.3 Å, the germline is around 4.3 Å, as reported previously in our previous paper.[10] Regarding the matured *R*-equatorial TS, the hydroxyl group is far away from the Glu-H35 but interacts with the Hsd-H96 instead. All in all, the only conformer that does not present a strong interaction between the hydroxyl group and any of the residues of the cavity, neither in the MC nor in the TS, is the *S*-axial which is, in fact, the one presenting the largest free energy barrier. Quite the reverse situation is shown by the *S*-equatorial; the lowest barrier is observed when the strongest interaction is established between the hydroxyl group and the Glu-H35 in the TS (1.89 Å) and this hydrogen bond is completely broken in MC (4.15 Å).

TABLE 1: Averaged Selected Internal Parameters over the Last 500 ps of 1 ns QM/MM Dynamics (Distances in Å and Angles in Degrees) of the TS and MC Obtained in the *S*-Axial, *S*-Equatorial, *R*-Axial, and *R*-Equatorial Conformers in Matured AZ28 Catalytic Antibody

	S-axial		*S*-equatorial		*R*-equatorial		*R*-axial	
	MC	TS	MC	TS	MC	TS	MC	TS
C1···C6	3.21	1.81	3.68	1.80	3.08	1.71	3.05	1.80
C3···C4	1.54	1.60	1.54	1.62	1.53	1.58	1.54	1.59
reaction coordinate	−1.67	−0.21	−2.14	−0.18	−1.55	−0.13	−1.51	−0.21
deviation from planarity								
internal ring		28.4		34.1		35.7		32.4
external ring		29.5		32.5		36.3		14.1
OH···Glu-H35	3.82	2.89	4.15	1.89	2.14	5.10	2.05	1.93
OH···Hsd-H96	5.51	5.72	5.09	4.38	3.42	2.53	3.51	4.38
OH···Asp-H101	5.17	5.51	7.98	7.16	6.88	7.78	7.14	6.91
Asp-H101···Asn-L34	2.64	2.18	2.66	2.01	2.02	2.45	2.01	2.13

The comparison of all the reactant complexes (MC in Table 1) shows that the pattern of interactions in *S*-axial and *R*-axial forms is maintained with respect to their corresponding TSs. As mentioned before, this is not the case in either the *S*-equatorial or the *R*-equatorial, where the hydroxyl group changes its interaction from MC to TS. In a different context, the change of the interaction pattern from MC to TS has been invoked as a plausible explanation of the lower catalytic efficiency of the mature antibody with respect to the germline.[10]

The analysis of the reaction coordinate, which is determined by the antisymmetric combination of the bonds that are being formed and broken ($d_{C3\cdots C4}-d_{C1\cdots C6}$), reveals that the smallest difference between the MC and the TS reaction coordinate is observed in the equatorial estereoisomers, being the *S*-equatorial the one presenting the largest difference. Obviously, this geometrical observation that, in principle, could be related to a lower free energy barrier in these conformers, seems to be less important than the effect of the interaction between the hydroxyl group and proton acceptor groups of the protein, previously discussed.

The substrate−CA interactions can be related to the QM/MM interaction energy term in our hybrid QM/MM scheme. Nevertheless, we must keep in mind that although free energy barriers obtained in terms of PMF have a quite credible magnitude, very long QM/MM dynamics are required to obtain a convergence in the interaction energies differences. Keeping this caution in mind, we have observed that the CA−substrate interaction is always higher in the TSs than in their corresponding reactant complexes, and thus the interaction energy difference between TS and reactants (ΔE_{int}) contributes to the lowering of the free energy barrier with respect to the uncatalyzed process. This trend is in agreement with the fact that the TS structures resembles to the TSA, which was the one used as hapten in the CA germline formation and maturation process. Furthermore, by comparison between the MC and TS, the maximum absolute value of the ΔE_{int} is obtained in the *S*-equatorial conformer, which corresponds with the lowest free energy barrier presenting process. The high value of the ΔE_{int} of the *S*-equatorial can be partially related to the short hydrogen bond distance between the hydroxyl group and the Glu-H35 residue in the TS, not present in the MC. Nevertheless, the analysis of the interaction energy differences of the rest of the conformers reveals that, although rendering much lower differences between MC and TS than in the *S*-equatorial case, a small difference in interaction energy between reactants and TS does not necessary imply a large free energy barrier. Obviously, this is not the unique term contributing to the potential energy barrier, as the reorganization of the CA and the energy of the substrate (the MM and the QM energy terms in the hybrid QM/MM scheme) have to be considered.

Another geometrical feature related to the reactivity of the system is the degree of planarity of the C2,C3,C1 and the C5,C4,C6 atoms, with their corresponding phenyl rings (external ring and internal ring, respectively). The radical character of the C2 and C5 atoms on the TS would be stabilized by electronic delocalization with the corresponding phenyl rings, which would increase if a planarity was reached. This electronic delocalization has been observed to be related to a diminution in the activation barriers in gas-phase calculations.[9] The relative position of the two phenyl rings with respect to the central ring has been measured in the TS by means of two dihedral angles listed in Table 1 that define the deviation from planarity of the external and internal rings ($\tau_{C5-C2-C1'-C2'}-90°$ and $\tau_{C2-C5-C1''-C2''}-90°$, respectively). In this sense, angles close to zero correspond to planarity whereas values around 90° would describe perpendicular orientations between the central ring and the external or the internal phenyl rings. These angles do not have a significant meaning in reactants, as long as the central ring is distorted with respect to the TS, but it can render some information in the TS, because the chairlike conformation in the central ring is only slightly deformed. The averaged values obtained in the TSs are close to 30°, indicating a considerable degree of planarity. It must be mentioned that the values obtained in the TSA were over 70°,[10] indicating much lower planarity than the TSs reported in Table 1. This feature must contribute to the catalytic efficiency of the CA by stabilizing the TS.

4. Discussion and Conclusions

We have studied in this paper the stereoselectivity of the oxy-Cope rearrangement in the AZ28 catalytic antibody: the preference for this reaction through a transition state with an axial or equatorial hydroxyl group orientation, and the capability of the AZ28 in differentiating between the R or S substrate stereoisomers.

By comparison of the CA matured forms, the free energy path trough a *S*-axial TS presents a barrier 2.6 kcal·mol^{-1} higher than the one through a *S*-equatorial TS. This trend was also obtained by Houk et al. by means of gas phase calculations, although showing that the *S*-axial was only 1 kcal·mol^{-1} higher in energy than the *S*-equatorial. This difference is increased when the interactions with the CA are considered in the simulations. One of the terms that can contribute to this increasing is the difference of substrate−CA interaction energy between reactants and TS. Nevertheless, a note of caution has to be introduced at this point, as this magnitude would require very long QM/MM dynamics to converge. Nevertheless, the most favored stereoisomer, the *S*-equatorial, presents the highest substrate−CA interaction energy difference.

The qualitative comparison of the barrier free energies obtained for all the different matured forms of the CA shows that although experimental trend has been reproduced in our simulations, the free energy difference between both S and R equatorial enantiomers does not match with a k_{cat}^S/k_{cat}^R ratio of 15:1 experimentally observed. This value corresponds to a difference in free energy barriers of 1.6 kcal·mol^{-1} at 300 K, far from our reported 0.2 kcal·mol^{-1}. Nevertheless, the analysis of the difference of interaction energies between reactants and TS for each conformer reveals that the increase in the case of the *S*-equatorial must be a key feature responsible of the fact that this conformation was the most favorable one, although it is not entirely reflected on the computed free energy barriers. We must keep in mind that the experimental difference of 1.6 kcal·mol^{-1} is, in fact, a very small difference and molecular dynamics carried out in theoretical simulations is always, at some extent, starting point dependent. Probably the *R*-equatorial conformer structure of the substrate docked in the X-ray initial structure of the CA was slightly closer to its absolute minimum energy structure than the *S*-equatorial stereoisomer. Anyway, the PMF traced for all the different possible stereoisomers, even if the initial guess structure was not an absolutely minimum in the PES, which would require very expensive long dynamic simulations, appears to be quite reliable and renders theoretical predictions in accordance with the experimental observations.

Finally, it is important to note that the difference between *S*-equatorial and *R*-equatorial, or between the *S*-axial and *R*-axial conformers, has been observed as a result of including the substrate−CA interactions in a flexible molecular model, allowing us to obtain different patterns of interactions that are related to different interaction energies. Thus, it has been observed that the hydroxyl group interacts quite strongly with the Glu-H35 residue in the *S*-equatorial TS, as in the TSA−CA complex, whereas in the *R*-equatorial TS the hydroxyl group interacts with a different residue, the His-H96, and no defined interaction is observed for the hydroxyl group in the *S*-axial orientation. This conformer presents, in fact, the less favorable free energy path. The pattern of interactions change from the TS to reactants in the *R*-equatorial enantiomer, but also in the *S*-equatorial TS. No clear interaction is established in the *S*-equatorial reactants and a new interaction with the Hsd-H96 is formed in the *R*-equatorial reactants. These changes observed in the *R*-equatorial and in the *S*-equatorial, could be partially responsibly of the loss of efficiency of the matured CA, with respect to the germline, as predicted in our previous paper.[10]

Acknowledgment. We are indebted to DGI for project DGI BQU2003-04168-C03, BANCAIXA for project P1A99-03 and Generalitat Valenciana for projects GV04B-021, GV04B-131 and GRUPOS04/08, which supported this research, and the Servei d'Informàtica of the Universitat Jaume I for providing us with computer capabilities.

References and Notes

(1) Raso, V.; Stollar, B. D. *Biochemistry* **1975**, *14*, 584−591.
(2) Keinan, E. *Catalytic Antibodies*; Wiley-VCH Verlag: Weinheim, 2005.
(3) Nossal, G. J. *Nature* **2003**, *421*, 440−444.
(4) Martí, S.; Roca, M.; Andrés, J.; Moliner, V.; Silla, E.; Tuñón, I.; Bertrán, J. *Chem. Soc. Rev.* **2004**, *33*, 98−107.
(5) Yin, J.; Schultz, P. G. Immunological Evolution of Catalysis. In *Catalytic Antibodies*; Keinan, E., Ed.; Wiley-VCH Verlag: Weinheim, 2005; Chapter 1, pp 1−29.
(6) Mader, M. M.; Bartlett, P. A. *Chem. Rev.* **1997**, *97*, 1281−1301.
(7) Ulrich, H. D.; Mundorff, E.; Santarsiero, B. D.; Driggers, E. M.; Stevens, R. C.; Schultz, P. G. *Nature* **1997**, *389*, 271−275.
(8) Asada, T.; Gouda, H.; Kollman, P. A. *J. Am. Chem. Soc*. **2002**, *124*, 12535−12542.
(9) Black, K. A.; Leach, A. G.; Yashar, M.; Kalani, S.; Houk, K. N. *J. Am. Chem. Soc.* **2004**, *126*, 9695−9708.
(10) Martí, S.; Andrés, J.; Moliner, V.; Silla, E.; Tuñón, I.; Bertrán, J. *Angew. Chem., Int. Ed.* **2005**, *44*, 904−909.
(11) Srinivasan, J.; Miller, J.; Kollman, P. A.; Case, D. A. *J. Biomol. Struct. Dyn.* **1998**, *16*, 671−682.
(12) Schultz, P. G.; Lerner, R. A. *Acc. Chem. Res.* **1993**, *26*, 391−395.
(13) Gouverneur, V. in, *Catalytic Antibodies*; Keinan, E., Ed.; Wiley-VCH Verlag: Weinheim, 2005; pp 370−417.
(14) Ulric, H. D.; Driggers, E. M. G.; Shultz, P. G. *Acta Chem. Scand.* **1996**, *50*, 328−332.
(15) Ulrich, H. D.; Shultz, P. G. *J. Mol. Biol.* **1998**, *275*, 95−111.
(16) Driggers, E. M.; Cho, H. S.; Liu, C. W.; Katzka, C. P.; Braisted, A. C.; Ulrich, H. D.; Wemmer, D. E.; Shultz, P. G. *J. Am. Chem. Soc.* **1998**, *120*, 1945−1958.
(17) Mundorff, E. C.; Hanson, M. A.; Varvak, A.; Ulrich, H.; Schultz, P. G.; Stevens, R. C. *Biochemistry* **2000**, *39*, 627−632.
(18) Jorgensen, W. L.; Maxwell, D. S.; Tirado-Rives, J. *J. Am. Chem. Soc.* **1996**, *118*, 11225−11236.
(19) (a) Field, M. J. *A practical Introduction to the Simulation of Molecular Systems*; Cambridge University Press: Cambridge, U.K., 1999. (b) Field, M. J.; Albe, M.; Bret, C.; Proust-de Martin, F.; Thomas, A. *J. Comput. Chem.* **2000**, *21*, 1088.
(20) Warshel, A. *Proc. Natl. Acad. Sci. U.S.A.* **1978**, *75*, 5250−5254.
(21) Torrie, G. M.; Valleau, J. P. *J. Comput. Phys.* **1977**, *23*, 187−199.
(22) Cornell, W. D.; Cieplak, P.; Bayly, C. I.; Gould, I. R.; Merz, K. M., Jr.; Ferguson, D. M.; Spellmeyer, D. C.; Fox, T.; Caldwell, J. W.; Kollman, P. A. *J. Am. Chem. Soc.* **1995**, *117*, 5179−5197.
(23) Martí, S.; Andrés, J.; Moliner, V.; Silla, E.; Tuñón, I.; Bertrán, J. *J. Phys. Chem B* **2000**, *104*, 11308−11315.
(24) Martí, S.; Andrés, J.; Moliner, V.; Silla, E.; Tuñón, I.; Bertrán, J.; Field, M. J. *J. Am. Chem. Soc.* **2001**, *123*, 1709−1712.